Springer

Journal of
Mechanical
Science and
Technology

Journal of Mechanical Science and Technology 23 (2009) 667~676

www.springerlink.com/content/1738-494x
DOI 10.1007/s12206-008-1117-y

A new method to evaluate the influence coefficient matrix for gas path analysis †

Di Xia*, Yonghong Wang and Shilie Weng

School of Mechanical Engineering, Shanghai Jiao Tong Univ., 800 Dong Chuan Rd. Shanghai 200240, P.R. China

(Manuscript Received May 23, 2008; Revised October 21, 2008; Accepted October 28, 2008)

Abstract

To create an online diagnostic system for a gas turbine, a well-formulated- influence coefficient matrix (ICM), a key component in a widely used existing theory, is essential. However, according to a recent research of the present authors, parameter deviations estimated by the traditional ICM contain unavoidable errors. These errors, called matching deviations, have been verified to be a consequence of the shifting operating point caused by component deterioration. Here we present a simple and accurate method which is still based on the widely accepted existing theory that accounts for component deterioration. Matching coefficients are introduced in this method to isolate and eliminate matching deviations. The ICM yielded by this method can improve the accuracy of both measurement prediction and parameter deviation estimations. By modeling a commercial power generation engine, a demonstration of the new method is presented and its limitation is discussed.

Keywords: Gas turbine; Influence coefficient matrix; Matching deviation

1. Introduction

Motivated by economics, a great number of gas turbines have been employed in power plants, a situation which then requires the development of monitoring and diagnostic systems. Since Urban [1-2] introduced his gas path analysis (GPA) in the 1970's, a substantial number of papers have been published in this area. These papers have proposed a wide variety of algorithms, employing linear [3] and non-linear methods [4], genetic algorithms [5-6], neural networks [7] and fuzzy expert systems [8-9]. Comparisons of these methods were extensively reviewed by Y. G. Li [10] and Kamboukos [11].

Currently, GPA is used in gas turbine analysis both widely and commercially. In considering the requirements for fast online diagnostic monitoring, a linear GPA method is utilized here.

The ICM, which is the key part of linear GPA, can be calculated by simultaneous difference equations, but its accuracy is limited. According to our recent research, engine degradation would lead to performance deteriorations of various components and a subsequent change in the operating point. Both performance deteriorations and change of the operating point would result in engine-independent parameter differences. However, only those parameter changes that have been induced directly by performance deterioration should be used to represent component degradation. Unfortunately, those parameter changes arising from changes in the operating point are also included in the simultaneous difference equations derived for the linear GPA method. We shall call these types of parameter differences matching deviations and illustrate in section 2 how they are eliminated in the analysis.

By incorporating this distinction, a new linear

† This paper was recommended for publication in revised form by Associate Editor Tong Seop Kim

*Corresponding author. Tel.: +86 21 13818464646, Fax.: +86 21 6447 0679
E-mail address: adi2088@msn.com

method is proposed to solve the above-mentioned problem, and demonstrated by modeling a PG9171E engine that has been running for the last twelve years at the Shanghai Zhadian Gas Turbine Power Plant. This method is also applicable to many other gas turbines.

The next section introduces the proposed gas path analysis method in detail. This is followed by a description of the engine model, while the applicability of the method is demonstrated in section 4.

2. Isolation and elimination of the matching deviations

In this section, matching deviations are investigated with the viewpoint of giving them a clear physical meaning, but also addressing their elimination.

As introduced by Urban, the following simultaneous difference equations exhibit the relationship between changes in measurements and independent parameter deviations of single spool turboshaft engines:

$$\delta\pi_T = \delta\pi_C + \delta\sigma_{in} + \delta\sigma_{out} + \delta\sigma_B \quad (1)$$

$$\delta W_C = K_1\delta\pi_C - \delta\eta_C \quad (2)$$

$$\delta W_T = \delta T_3 + K_3\delta\pi_T + \delta\eta_T \quad (3)$$

$$\delta T_2 = K_1K_2\delta\pi_C - K_2\delta\eta_C \quad (4)$$

$$\delta T_4 = \delta T_3 - K_3K_4\delta\pi_T - K_4\delta\eta_T \quad (5)$$

$$\delta G_C = \delta\overline{G^*_C} + \delta\sigma_{in} \quad (6)$$

$$\delta\overline{G^*_T} = \delta G_T + \frac{1}{2}\delta T_3 - \delta\pi_C - \delta\sigma_{in} - \delta\sigma_B \quad (7)$$

$$\delta W_F = \delta G_C + K_5\delta T_3 - (K_5-1)\delta T_2 - \delta\eta_B \quad (8)$$

$$\delta NE = \delta G_C + K_6\delta W_T - (K_6-1)\delta W_C \quad (9)$$

where we have employed the following definitions:

$$m_1 = \frac{(K_C-1)}{K_C}, m_2 = \frac{(K_T-1)}{K_T}; K_1 = \frac{m_1\pi_C^{m_1}}{\pi_C^{m_1}-1};$$

$$K_2 = \frac{\pi_C^{m_1}-1}{\pi_C^{m_1}-1+\eta_C}; K_3 = \frac{m_2}{\pi_T^{m_2}-1}; K_4 = \frac{(\pi_T^{m_2}-1)\eta_T}{\pi_T^{m_2}-(\pi_T^{m_2}-1)\eta_T};$$

$$K_5 = \frac{(1+f)T_3}{(1+f)T_3 - T_2}; K_6 = \frac{(1+f)G_C W_T}{(1+f)G_C W_T - W_C}$$

Rearrangement of Eq. (4) gives

$$-K_1K_2\delta\pi_C + \delta T_2 = -K_2\delta\eta_C \quad (10)$$

and by inserting Eqs. (1), (6) and (8) into Eq. (5) for a given operating point ($\delta W_F = 0$), we obtain,

$$\begin{aligned} &K_3K_4\delta\pi_C - \frac{(K_5-1)}{K_5}\delta T_2 + \delta T_4 \\ &= -\frac{1}{K_5}\delta\overline{G^*_C} - K_4\delta\eta_T + \frac{1}{K_5}\delta\eta_B - (\frac{1}{K_5} + K_3K_4)\delta\sigma_{in} \\ &\quad -K_3K_4\delta\sigma_{out} - K_3K_4\delta\sigma_B \end{aligned} \quad (11)$$

Substitution of Eqs. (6) and (8) into Eq. (7) gives

$$\begin{aligned} &\delta\pi_C - \frac{(K_5-1)}{2K_5}\delta T_2 \\ &= (1-\frac{1}{2K_5})\delta\overline{G^*_C} - \delta\overline{G^*_T} + (\frac{1}{2K_5} - 1)\delta\eta_B - \frac{1}{2K_5}\delta\sigma_{in} \end{aligned} \quad (12)$$

while insertion of Eqs. (1), (2), (3), (6) and (8) into Eq. (9) yields

$$\begin{aligned} &\delta NE + [(K_6-1)K_1 - K_6K_3]\delta\pi_C - \frac{K_6(K_5-1)}{K_5}\delta T_2 \\ &= (1-\frac{K_6}{K_5})\delta\overline{G^*_C} + (K_6-1)\delta\eta_C + K_6\delta\eta_T + \frac{K_6}{K_5}\delta\eta_B \\ &\quad + (1-\frac{K_6}{K_5} + K_6K_3)\delta\sigma_{in} + K_6K_3\delta\sigma_{out} + K_6K_3\delta\sigma_B \end{aligned} \quad (13)$$

To calculate the ICM, Eqs. (1-9) can be expressed in matrix form:

$$\begin{bmatrix} 0 & -K_1K_2 & 1 & 0 \\ 0 & K_3K_4 & -\frac{(K_5-1)}{K_5} & 1 \\ 0 & 1 & -\frac{(K_5-1)}{2K_5} & 0 \\ 1 & [(K_6-1)K_1-K_6K_3] & -\frac{K_6(K_5-1)}{K_5} & 0 \end{bmatrix} \bullet \begin{bmatrix} \delta NE \\ \delta\pi_C \\ \delta T_2 \\ \delta T_4 \end{bmatrix} =$$

$$\begin{bmatrix} 0 & -K_2 & 0 & 0 & 0 & 0 & 0 & 0 \\ -\frac{1}{K_5} & 0 & 0 & -K_4 & \frac{1}{K_5} & -(\frac{1}{K_5}+K_3K_4) & -K_3K_4 & -K_3K_4 \\ (1-\frac{1}{2K_5}) & 0 & -1 & 0 & (\frac{1}{2K_5}-1) & -\frac{1}{2K_5} & 0 & 0 \\ (1-\frac{K_6}{K_5}) & (K_6-1) & 0 & K_6 & \frac{K_6}{K_5} & (1-\frac{K_6}{K_5}+K_6K_3) & K_6K_3 & K_6K_3 \end{bmatrix} \bullet \begin{bmatrix} \delta\overline{G^*_C} \\ \delta\eta_C \\ \delta\overline{G^*_T} \\ \delta\eta_T \\ \delta\eta_B \\ \delta\sigma_{in} \\ \delta\sigma_{out} \\ \delta\sigma_B \end{bmatrix} \quad (14)$$

which can be simplified as

$$\delta\vec{\mathbf{m}} = \mathbf{S}\cdot\delta\vec{\mathbf{p}} \quad (15)$$

by defining row vectors

$$\delta\mathbf{m}^{\mathrm{T}} = \left(\delta NE \quad \delta\pi_C \quad \delta T_2 \quad \delta T_4\right)$$

$$\delta\mathbf{p}^{\mathrm{T}} = \left(\delta\overline{G_C^*} \quad \delta\eta_C \quad \delta\overline{G_T^*} \quad \delta\eta_T \quad \delta\eta_B \quad \delta\sigma_{in} \quad \delta\sigma_{out} \quad \delta\sigma_B\right)$$

And the rectangular diagnostics matrix S (see Table 1) can be then evaluated for the design point (P0=0.101MPa, T0=288K, WF=9.25kg/s). To obtain the square matrix for our study, the parameter differences $\delta\eta_B, \delta\sigma_{in}, \delta\sigma_{out}, \delta\sigma_B$ are assumed to be zero.

The parameter deviations estimated by Eq. (15) are of two types: Type I corresponds to the change in the characteristic map which is induced by engine degradation, and will lead to a change in the operating point. Type II corresponds to effects of the matching procedure brought about by a change of operating point.

Obviously, these two types are not independent of each other. Those effects ascribed to Types II that are induced by changes attributed to Type I do not represent performance degradation and should be eliminated from the parameter deviation estimated by the ICM S. To illustrate the physical meanings of these two parts, we present in Fig. 1 the characteristics of the compressor.

The shift in the characteristic map is due to fouling in the compressor blade, which leads to losses of pressure ratio, compressor efficiency, and flow capacity. In Fig.1, Point A is the design point of a new engine while the nominal speed line is $\overrightarrow{\mathbf{QBA}}$. Also, Point B' indicates the design point of the deteriorated engine and $\overrightarrow{\mathbf{Q'B'A'}}$ is the new nominal speed line.

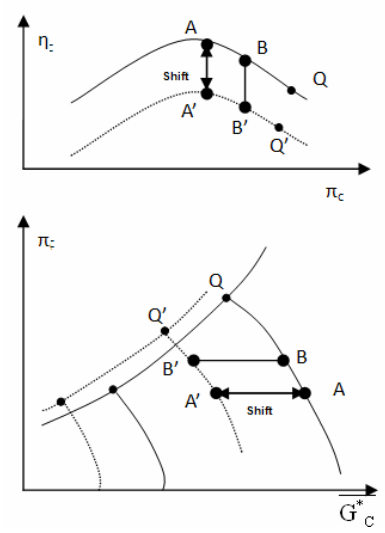

Fig. 1. Illustration of matching deviation.

The losses associated with both corrected mass flow and efficiency at the design point can be expressed as follows:

$$\delta\overline{G^*_c} = \delta\overline{G^*_{C(B'A)}} = \delta\overline{G^*_{C(B'A')}} + \delta\overline{G^*_{C(A'A)}} \tag{16}$$

$$\delta\eta_c = \delta\eta_{C(B'A)} = \delta\eta_{C(B'A')} + \delta\eta_{C(A'A)} \tag{17}$$

where:

$$\delta\overline{G^*_{C(B'A)}} = \frac{\overline{G^*_{C(B')}} - \overline{G^*_{C(A)}}}{\overline{G^*_{C(A)}}}; \delta\overline{G^*_{C(B'A')}} = \frac{\overline{G^*_{C(B')}} - \overline{G^*_{C(A')}}}{\overline{G^*_{C(A)}}};$$

$$\delta\overline{G^*_{C(A'A)}} = \frac{\overline{G^*_{C(A')}} - \overline{G^*_{C(A)}}}{\overline{G^*_{C(A)}}}; \delta\eta_{C(B'A)} = \frac{\eta_{C(B')} - \eta_{C(A)}}{\eta_{C(A)}};$$

$$\delta\eta_{C(B'A')} = \frac{\eta_{C(B')} - \eta_{C(A')}}{\eta_{C(A)}}; \delta\eta_{C(A'A)} = \frac{\eta_{C(A')} - \eta_{C(A)}}{\eta_{C(A)}}$$

$$\pi_{C(B)} = \pi_{C(B')}; \pi_{C(A)} = \pi_{C(A')}$$

Herein, $\delta\overline{G^*_{C(A'A)}}$ and $\delta\eta_{C(A'A)}$ are called characteristic deviations as determined by the definition of Type I and would lead to a new operating point, which is then matched through the deteriorated components. Incorporating these characteristic deviations into the matching procedure results in matching deviations $\delta\overline{G^*_{C(B'A')}}$ and $\delta\eta_{C(B'A')}$. In a previous work [2] $\delta\overline{G^*_{C(B'A)}}$ and $\delta\eta_{C(B'A)}$, as estimated by Eq. (15), are used to express the degree of degradation. The problem to be solved here is to present a new method to evaluate the ICM. Parameter deviations estimated from this ICM should be precisely the characteristic deviations such as $\delta\overline{G^*_{C(A'A)}}$ and $\delta\eta_{C(A'A)}$.

The curve $\overrightarrow{\mathbf{QBA}}$ in Fig. 1 can be described as a function of π_C : $\overline{G^*_C} = \varphi_C(\pi_C)$ and $\eta_C = \phi_C(\pi_C)$. The matching deviations can then be expressed as:

$$\delta\overline{G^*_{C(B'A')}} \cong \delta\overline{G^*_{C(BA)}} = K_{gc}\delta\pi_{C(BA)} = K_{gc}\delta\pi_{C(B'A)} \tag{18}$$

$$\delta\eta_{C(B'A')} \cong \delta\eta_{C(BA)} = K_{ec}\delta\pi_{C(BA)} = K_{ec}\delta\pi_{C(B'A)} \tag{19}$$

Here K_{gc} and K_{ec} are called matching coefficients. They are gradients determined at the operating point A of curve $\overrightarrow{\mathbf{QBA}}$ and defined as:

$$K_{gc} = \left[\frac{\delta\varphi(\pi_c)}{\delta\pi_c}\right]_A; K_{ec} = \left[\frac{\delta\phi(\pi_c)}{\delta\pi_c}\right]_A$$

Substituting Eq. (18) into Eq. (16) and Eq. (19) into Eq. (17) we have:

Table 1. Coefficients of diagnostic matrix S.

	$\delta\overline{G_C^*}$	$\delta\eta_C$	$\delta\overline{G_T^*}$	$\delta\eta_T$	$\delta\sigma_B$	$\delta\sigma_{in}$	$\delta\sigma_{ex}$	$\delta\sigma_B$
δNE	-0.0015	0.5472	-0.358	2.087	1.23	0.434	0.663	0.908
$\delta\pi_C$	0.7805	-0.128	-1.071	0	0.291	-0.291	0	-0.929
δT_2	0.227	-0.558	-0.311	0	0.085	-0.085	0	-0.27
δT_4	-0.616	-0.226	0.101	-0.714	0.515	-0.742	-0.227	0.126

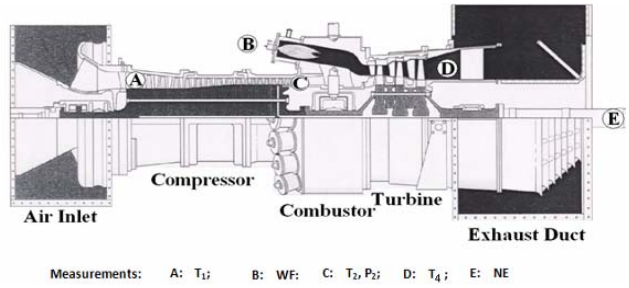

Fig. 2. Schematic diagram of a PG9171E gas turbine.

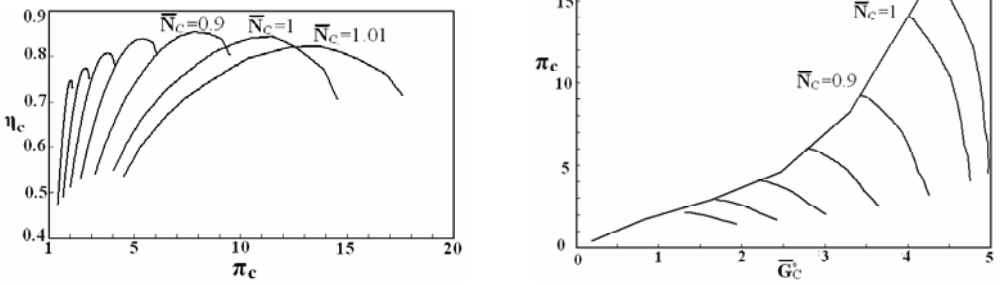

Fig. 3. Characteristics of compressor.

$$\delta\overline{G^*_C}=\delta\overline{G^*_{C(B'A)}}=K_{gc}\delta\pi_{C(B'A)}+\delta\overline{G^*_{C(A'A)}} \quad (20)$$

$$\delta\eta_C=\delta\eta_{C(B'A)}=K_{ec}\delta\pi_{C(B'A)}+\delta\eta_{C(A'A)} \quad (21)$$

$$\delta\pi_{C(B'A)}=\frac{\pi_{C(B')}-\pi_{C(A)}}{\pi_{C(A)}}$$

where

In a similar manner, the turbine deviations can be expressed as:

$$\delta\overline{G^*_T}=\delta\overline{G^*_{T(B'A)}}=K_{gt}\delta\pi_{T(B'A)}+\delta\overline{G^*_{T(A'A)}} \quad (22)$$

$$\delta\eta_T=\delta\eta_{T(B'A)}=K_{et}\delta\pi_{T(B'A)}+\delta\eta_{T(A'A)} \quad (23)$$

where:

$$\overline{G^*_T}=\varphi_T(\pi_T);\eta_T=\phi_T(\pi_T)$$

$$\delta\overline{G^*_{T(B'A)}}=\frac{\overline{G^*_{T(B')}}-\overline{G^*_{T(A)}}}{\overline{G^*_{T(A)}}};\ \delta\overline{G^*_{T(A'A)}}=\frac{\overline{G^*_{T(A')}}-\overline{G^*_{T(A)}}}{\overline{G^*_{T(A)}}}$$

$$\delta\eta_{T(B'A)}=\frac{\eta_{T(B')}-\eta_{T(A)}}{\eta_{T(A)}};\ \delta\eta_{T(A'A)}=\frac{\eta_{T(A')}-\eta_{T(A)}}{\eta_{T(A)}}$$

$$\delta\pi_{T(B'A)}=\frac{\pi_{T(B')}-\pi_{T(A)}}{\pi_{T(A)}};\ K_{gt}=\left[\frac{\delta\varphi_T(\pi_T)}{\delta\pi_T}\right]_A;\ K_{et}=\left[\frac{\delta\phi_T(\pi_T)}{\delta\pi_T}\right]_A$$

By inserting Eqs. (20)-(23) into Eq. (15), we can get a new set of simultaneous difference equations:

$$\begin{bmatrix} 0 & (K_2K_m-K_3K_2) & 1 & 0 \\ 0 & (K_4K_m+\frac{K_g}{K_5}+K_3K_4) & -\frac{(K_5-1)}{K_5} & 1 \\ 0 & [1-(1-\frac{1}{2K_5})K_g+K_g] & -\frac{(K_5-1)}{2K_5} & 0 \\ 1 & [(K_6-1)K_3-K_6K_3-(1-\frac{K_6}{K_5})K_g-(K_6-1)K_m-K_6K_m] & -\frac{K_6(K_5-1)}{K_5} & 0 \end{bmatrix} \bullet \begin{bmatrix} \delta NE \\ \delta\pi_C \\ \delta T_2 \\ \delta T_4 \end{bmatrix} = \begin{bmatrix} 0 & -K_2 & 0 & 0 & 0 & 0 & 0 & 0 \\ -\frac{1}{K_5} & 0 & 0 & -K_4 & \frac{1}{K_5} & -(\frac{1}{K_5}+K_3K_4+K_4K_m) & -(K_3K_4+K_4K_m) & -(K_3K_4+K_4K_m) \\ (1-\frac{1}{2K_5}) & 0 & -1 & 0 & (\frac{1}{2K_5}-1) & -(\frac{1}{2K_5}+1) & -1 & -1 \\ (1-\frac{K_6}{K_5}) & (K_6-1) & 0 & K_6 & \frac{K_6}{K_5} & (1-\frac{K_6}{K_5}+K_6K_3+K_6K_m) & (K_6K_3+K_6K_m) & (K_6K_3+K_6K_m) \end{bmatrix} \bullet \begin{bmatrix} \delta\overline{G^*_{C(A'A)}} \\ \delta\eta_{C(A'A)} \\ \delta\overline{G^*_{T(A'A)}} \\ \delta\eta_{T(A'A)} \\ \delta\eta_B \\ \delta\sigma_m \\ \delta\sigma_{out} \\ \delta\sigma_B \end{bmatrix} \quad (24)$$

and consequently a new diagnostic matrix S'(see Table 2).

3. PG9171E engine model

The PG9171E engine (see Fig. 2) with 113.790-MW output capacity consists of a multistage axial compressor, a fourteen-chamber combustion system, and a three-stage axial turbine. To establish a sufficiently accurate engine model [14], two simplifying methods were adopted in determining the component characteristics. Characteristics of the compressor (see Fig. 3) were determined by Qin's method [15, 16], which is based on experimental data of eight axial-flow compressors. The Kotlial algorithm-based inverse computation method [17] was adopted to determine characteristics of the turbine. With the characteristics determined, an engine model (see Fig.4) was created and modified with experimental data obtained in 1997 when the engine was commissioned. Constant standard values were used for the gear box efficiency, spool speed, cooling air consumption, and inlet and outlet parameters of the air cooler. Given the fuel mass flow rate, inlet temperature and pressure, our engine model is able to provide performance parameters and measurement evaluations. Table 3 shows model outputs and measured values agree very well.

Table 2. Coefficients of diagnostic matrix S'.

	$\delta\overline{G_{C(A'A)}}^*$	$\delta\eta_{C(A'A)}$	$\delta\overline{G_{T(A'A)}}^*$	$\delta\eta_{T(A'A)}$
δNE	-0.163	0.559	-0.223	2.087
$\delta\pi_C$	0.630	-0.0929	-0.965	0
δT_2	0.2245	-0.557	-0.308	0
δT_4	-0.472	-0.220	-0.077	-0.714

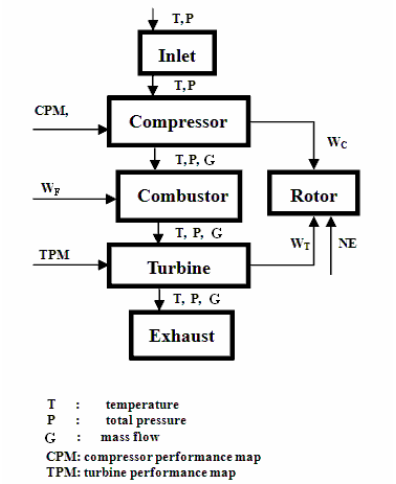

Fig. 4. Flow diagram of model components.

Table 3. Comparisons of measurements to engine model results.

	P_0(MPa)	0.101	0.101	0.102	0.101
	T_0(K)	285	290	292	288
	W_F(kg/s)	5.09	7.33	8.04	9.25
NE(MW)	Test data	40	70	80	100
	Model result	40.23	70.36	79.5	100.899
	Relative error (%)	-0.575	-0.514	0.625	-0.899
T_4(K)	Test data	643.7	678.2	710.4	772.1
	Model result	642	679.9	712.6	770.9
	Relative error (%)	0.265	-0.270	-0.318	0.148
P_2(MPa)	Test data	0.77	0.972	0.986	1.048
	Model result	0.774	0.970	0.979	1.039
	Relative error (%)	-0.475	0.205	0.73108	0.885

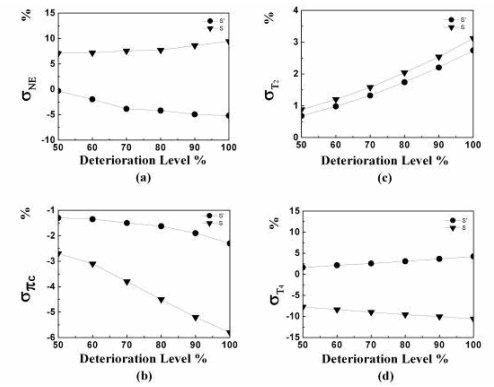

Fig. 5. Measurement prediction errors of ICM S and S'.

4. Measurement determination and parameter estimation

To evaluate the new method, the ICMs S' and S were applied to real-time operation data from 15 Dec 2007 for the PG9171E engine. According to the power plant operation history, the compressor water wash had been performed six times during the period May to October of 2007, but was discontinued from October 10th for nearly three months. The evaluation report from the GE Company indicated that characteristic deviations of the engine are $\delta\overline{G_C^*}$ =-10.173%, $\delta\eta_C$ =-3.491%, $\delta\overline{G_T^*}$ =1.532%, $\delta\eta_T$ =-3.213%. As shown in Appendix A, calculated values in this report come from a nonlinear GPA method [18].

Some of the known deterioration mechanisms are fouling and erosion, clearance increases, and other primary and secondary flow leaks. After evaluating analytic engine teardowns, production test data, development test data, and overhaul engine findings, it was determined that the rotating component efficiencies and flow parameters are affected by deterioration [19]. The outcome of these analyses is an empirical engine deterioration model that represents a relationship between a variety of module health parameters and quantitative engine deterioration levels [20-23]. Four engine-health parameters are identified for the engine deterioration model considered in this paper. Table 4 shows changes of these parameters corresponding to given fault conditions. With Table 4 and characteristic deviations estimated in the GE report, severe compressor fouling of the engine was predicted by the plant operator.

Table 4. Fault criteria for single-fault of gas turbine.

Fault conditions	Parameter changes	
Compressor fouling	$\delta\overline{G_c^*}$=-7%	$\delta\eta_c$=-2%
Compressor tip clearance increases	$\delta\overline{G_c^*}$=-4%	
Compressor erosion		$\delta\eta_c$=-2%
Compressor foreign object damage	$\delta\overline{G_c^*}$=-1%	$\delta\eta_c$=-5%
Turbine erosion	$\delta\overline{G_T^*}$=4%	
Turbine fouling	$\delta\overline{G_T^*}$=-6%	$\delta\eta_T$= 2%
Turbine Abrasion	$\delta\overline{G_T^*}$= 6%	$\delta\eta_T$=-2%
Turbine foreign object damage		$\delta\eta_T$=-5%

Given the fault case mentioned above, $\delta\vec{\mathbf{m}}$ can be evaluated by ICM S' and S. Fig. 5 shows the relative errors between the ICM based $\delta\vec{\mathbf{m}}$ and the engine model based $\delta\vec{\mathbf{m}}^*$. Reference operating points used in Fig. 5 are design points that were calculated by the engine model assuming different levels of degradation. With respect to Fig. 5, the extreme values of the deterioration level are defined as:

Deterioration Level = 0%: A new engine without any deterioration with corresponding health parameters ($\delta\overline{G_C^*}$ =0%, $\delta\eta_C$ =0%, $\delta\overline{G_T^*}$ =0%, $\delta\eta_T$ =0%);

Deterioration Level = 100%: a fully deteriorated

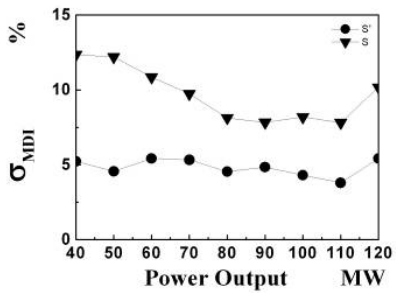

Fig. 6. Comparison of σ_{MDI} at different loads.

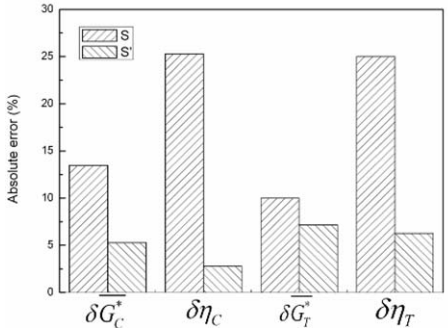

Fig. 7. Comparison of estimation results of ICM S and S' with model data.

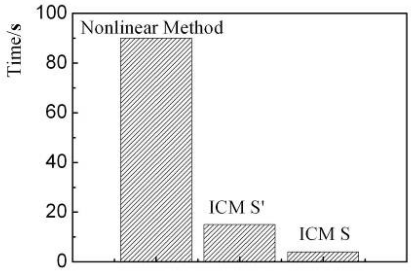

Fig. 8. Comparison of diagnostic methods in terms of computation speed.

engine with corresponding health parameters ($\delta\overline{G_C^*}$ =-10.173%, $\delta\eta_C$ =-3.491%, $\delta\overline{G_T^*}$ =1.532%, $\delta\eta_T$ =-3.213%).

To analyze the influence of matching coefficients at different load conditions on model accuracy, the ICMs S and S' were calculated for nine various operating conditions. Fig. 6 shows measurement prediction errors for these matrices for a fully deteriorated engine. The indicator σ_{MDI} in Fig.6 is defined as:

$$\sigma_{MDI} = \sqrt{\frac{\sigma_{NE}^2 + \sigma_{T_2}^2 + \sigma_{T_4}^2 + \sigma_{\pi_C}^2}{4}} \tag{25}$$

The influence of matching deviations on parameter estimation is also examined. Given characteristic deviations used above, measurements could be generated by the engine model. They are then provided as an input for ICMs S and S' used to perform the estimations. The results of the analysis are compared with data from the GE report, and the absolute errors are shown in Fig.7. Fig.8 shows a comparison of the overall run-times for various diagnostic methods taken for the PG9171E engine. The nonlinear-based diagnostics model took one-and-a-half minutes for convergence, while our new linear method took about 15 seconds to establish a solution. The new method is six times faster than the nonlinear method within practical accuracy limits. In the case of single fault diagnosis, two cases: ($\delta\overline{G_C^*}$ =-10.173%, $\delta\eta_C$ =-3.491%, $\delta\overline{G_T^*}$ =0%, $\delta\eta_T$ =0% and $\delta\overline{G_C^*}$ =0%, $\delta\eta_C$ =0%, $\delta\overline{G_T^*}$ =1.532%, $\delta\eta_T$ =-3.213%) were utilized. As illustrated in Fig. 9, the accuracy of single fault diagnostics is also improved by the new method.

As seen in this section, application of the ICM S' indicates a great improvement in accuracy. It also verifies that the omission of K_{gc}, K_{ec}, K_{gt}, and K_{et} is the main reason for the errors arising in the traditional set of simultaneous equations.

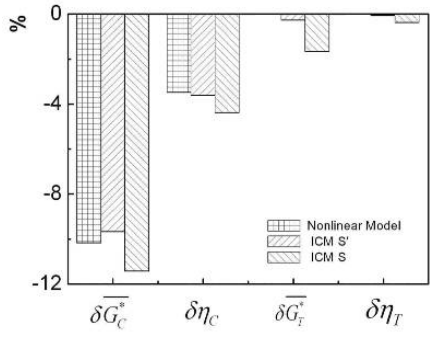

(a)

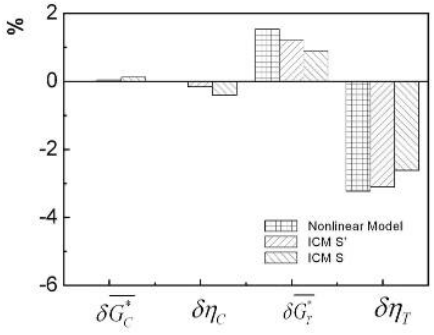

(b)

Fig. 9. Single fault diagnostic results for the nonlinear method and ICMs.

5. Discussion

As shown in Fig.6, the effects of K_{gc}, K_{ec}, K_{gt}, and K_{et} on the accuracy of measurement determination varies with different load conditions. During load reduction, the compressor pressure ratio π_C decreases correspondingly. Therefore, values of the slope coefficients K_{gc}, K_{ec}, K_{gt}, and K_{et} of the operating point would change. For example, the values of K_{gc}, K_{ec}, K_{gt}, and K_{et} are -0.11,0.008,0,-0.00044, respectively, while the fault free engine had been operating at 100 MW output power. When the load decreased to 40 MW, K_{gc}, K_{ec}, K_{gt}, and K_{et} would change to -0.046, 0.038, 0.0000012, 0.0014, respectively. Fig. 6 shows the influence of these changes on measurement prediction accuracy. The Shanghai Zhadian Gas Turbine Power Plant is a peak-shaving plant for which 40MW load is the normal load condition during the engine operating process (see Fig.10).

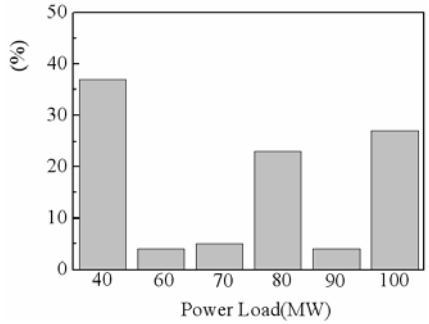

Fig. 10. Classification of load conditions for the PG9171E engine in 2007.

The application of ICM S at 40 MW load would result in values of σ_{MDI} of more than twelve percent. However, the new method can greatly decrease these values of σ_{MDI} to less than five percent.

To reduce the model to a square ICM matrix problem, $\delta\eta_B$, $\delta\sigma_{in}$, $\delta\sigma_{out}$, $\delta\sigma_B$ and the changes of other parameters were assumed to be zero. In most situations they will not remain unchanged, so in future research, nonzero values should be considered. However, to solve this reduced problem, the most direct way is to include some measurements such as compressor mass flow readings. Then, in this case, $\delta\eta_B$ can be calculated by the ICM, and other parameters such as $\delta\sigma_{in}$, $\delta\sigma_{out}$, $\delta\sigma_B$ can be set constant by testing data during maintenance. However, the taking of measurements is usually not permitted by the vendor for safety reasons. Therefore, a method has been introduced to overcome the deficiency of measurements over parameters [24]. The idea behind this method is to exploit data from existing sensors at several discrete operating points to obtain a greater number of parameters. Different research groups have appreciated the potential of this method, and its implementation in different situations has been the subject of recent studies [25-27]. This technique, at least in the situations it has been recently implemented, is rather efficient when the operating points are clearly discrete, namely, when they are far apart in the engine-operating envelope. Inefficiencies for closely-spaced operating points were observed by Groenstedt [26], while Gulati et al. [27] also identified similar inadequacies in their implementation.

The linear GPA method utilized here relies on the assumption of linearity and is only acceptable for very small ranges of values of the influential parameters about the operating condition. The nonlinearity consists in the fact that measured variables and parameters are interrelated not through simplified linear relations, but through a fully nonlinear thermodynamic model. Therefore, the assumption of linearity would become increasingly inaccurate when deteriorations cause the engine to operate further away from the operating point for which the matrix was calculated. This inadequacy of the linear method has led to non-linear methods being devised. However, these methods need much more computational resources and have a much slower execution time. To solve this problem, a tentative idea of the present authors is to present a combinatorial approach, in which matching coefficients are applied in the non-linear method. Instead of calculating parameter changes (such as $\overline{\delta G^*_{T(B'A)}} = (\overline{G^*_{T(B')}} - \overline{G^*_{T(A)}}) / \overline{G^*_{T(A)}}$) by ICM, health parameters of a fault-free engine (such as $\overline{G^*_{T(A)}}$) and a deteriorating engine (such as $\overline{G^*_{T(B')}}$) could be calculated by a fault-free engine model and a thermodynamic cycle calculation model, respectively, by using this combinatorial method. The real characteristic deviations (such as $\overline{\delta G^*_{T(A'A)}}$) can then be obtained by elimination of matching deviations in $\overline{\delta G^*_{T(B'A)}}$. A preliminary result shows that this method has almost the same accuracy with the non-linear method, and the computational load is reduced by a half. An application of this combinatorial approach will be described in a forthcoming paper by the authors.

6. Conclusions

A novel method for improving the diagnostic accuracy of the linear GPA method was presented. The method is applicable to situations where data are available at steady operating conditions and can increase both the accuracy of measurement determination and parameter deviation estimation. In this method, matching coefficients, which are capable of matching deviation elimination, are implemented during the calculation of the ICM.

The new method was tested against both measurement determinations and parameter deviation estimations, with an implementation set typical for current PG9171E engines. It was found that the method could detect and identify correctly faults in compressor and turbine, with greater accuracy than the traditional ICM approach.

In this study, due to the limited number of measurements, only four parameters were considered in the new method. It is straightforward to extend the algorithm to include the combustor efficiency or pressure loss deviation by methods incorporating multiple operating point analysis.

Nomenclature

f : Fuel-air ratio
T_2 : Compressor outlet temperature(K)
G_C : Compressor mass flow rate(t/hr)
T_3 : Turbine inlet temperature(K)

$\overline{G^*_C}$: Corrected compressor mass flow rate
T_4 : Turbine outlet temperature(K)
G_T : Turbine mass flow rate(t/hr)
W_C : Compressor power(MW)
$\overline{G^*_T}$: Corrected turbine mass flow rate
W_F : Fuel mass flow rate(kg/s)
ICM : Influence coefficient matrix
W_T : Turbine power(MW)
K_C : Adiabatic exponent of compressor
Δ : The normalized deviation from the nominal value
K_T : Adiabatic exponent of turbine
η_B : Combustor efficiency
$\tilde{\mathbf{m}}$: Measurable dependent parameters
η_C : Compressor efficiency
NE : Generator power(MW)
η_T : Turbine efficiency
$\overline{N_C}$: Nominal speed line of compressor
π_C : Compressor pressure ratio
$\tilde{\mathbf{p}}$: Unmeasurable independent parameters
π_T : Turbine compressor pressure ratio
P_0 : Ambient pressure(MPa)
Σ : Relative error
P_2 : Compressor discharge pressure(MPa)
σ_B : Total pressure loss in the combustor(%)
T_0 : Ambient temperature(K)
σ_{in} : Inlet pressure loss(%)
T_1 : Compressor inlet temperature(K)
σ_{out} : Outlet pressure loss(%)

References

[1] L. A. Urban, Parameter selection for multiple fault diagnostics of gas turbine engines, *AGARD Conference Proceedings*, Liege, Belgium (1974).

[2] L. A. Urban, Gas path analysis of commercial aircraft engines. *Proceedings of the 11th Symposium on Aircraft Integrated Data Systems*, Cologne, West Germany (1982).

[3] D. L. Doel, TEMPER - a gas-path analysis tool for commercial jet engines, *Journal of Engineering for Gas Turbines and Power* 116 (1) (1994) 82-89.

[4] A. Stamatis, K. Mathioudakis and M. Smith M, Gas turbine component fault identification by means of adaptive performance modeling, *Proceedings of ASME Turbo Expo*, Brussels, Belgium (1990)90-GT-376.

[5] M. Zedda and R. Singh, Gas-turbine engine and sensor diagnostics, *XIV International symposium on air-breathing engines*, Florence, Italy.(1999)255-261.

[6] M. Zedda and R. Singh, Gas turbine engine and sensor fault diagnosis using optimization techniques, *Journal of Propulsion and Power* 18 (5) (2002) 1019-1025.

[7] G. Denny, F-16 Jet Engine Trending and Diagnostics with Neural Networks, *Applications of Neural Networks* 4(1965) 419-422.

[8] P. Fuster, A. Ligeza and M. J. Aguilar, Abductive diagnostic procedure based on an AND/OR/NOT graph for expected behaviour: Application to a gas turbine, *10th International Congress and Exhibition on Condition Monitoring and Diagnostic Engineering Management*, Helsinki, Finland. (1997).

[9] C. Siu, Q. Shen and R. Milne, TMDOCTOR: A fuzzy rule-and case-based expert system for turbomachinery diagnosis, *Proceedings of IFAC Fault Detection, Supervision and Safety for Technical Processes*, Kingston Upon Hull, UK. (1997).

[10] Y. G. Li, Performance-analysis-based gas turbine diagnostics: A review, *Proceedings of the Institution of Mechanical Engineers, Part A: Journal of Power and Energy* 216 (5)(2002)363-377.

[11] P. Kamboukos and K. Mathioudakis, Comparison of linear and nonlinear gas turbine performance diagnostics. *Journal of Engineering for Gas Turbines and Power* 127 (1) (2005) 49-56.

[12] M. Naeem, R. Singh and D. Probert, Consequence of areo-engine deteriorations for military aircraft, *Applied Energy* 70(3) (2001) 103-133.

[13] M. Kurosaki, T. Morioka and K. Ebina, Fault detection and identification in an IM270 gas turbine using measurements for engine control, *Journal of Engineering for Gas Turbines and Power* 126 (4) (2004) 726-732.

[14] D. Xia and Y. H. Wang, Modeling for the calculation of off-design operating conditions of a model PG9171E gas turbine, *Journal of Engineering for Thermal Energy and Power*, 4(2008) 15-18.

[15] P. Qin, *Aerodynamic Design of Axial Flow Compressor*, National Defence Industry Press, Beijing, 214-235(1975).

[16] A. R. Howell and R. P. Bonham, Over-all and stage characteristics of axial flow compressors, *Proceedings of the Institution of Mechanical Engineers*, 163(1950) 235-248.

[17] Y. H. Wang, A new method of predicting the performance of gas turbine engines, *Journal of Engineering for Gas Turbines and Power*, 113(1991) 106-111.

[18] A. Stamatis, K. Mathioudakis and K. D. Papailiou, Adaptive simulation of gas turbine performance. *Journal of Engineering for Gas Turbines and Power*, 112 (1990) 168-175.

[19] R. T. Rausch, K. F. Goebel, N. H. Eklund and B. J. Brunell, Integrated in-flight fault detection and accommodation: a Model-based study, *Proceedings of ASME Turbo Expo*, Reno, Nevada, USA (2005) 05-GT-68300.

[20] H. I. H. Saravanamuttoo, Gas path analysis for pipeline gas turbines. *1st Canadian Symposium on Gas Turbine Operation and Maintenance*, USA, (2005).

[21] Z. Ping and S. Hih, Simulation of an advanced twin-spool industrial gas turbine, *ASME Journal of Engineering for Gas Turbines and Power*, 114 (1992) 180-186.

[22] K. Mathioudakis and A. Tsalavoutas, Uncertainty reduction in gas turbine performance diagnostics by accounting for humidity effects. *Proceedings of ASME Turbo Expo*, New Orleans, USA (2001) 01-GT-0010.

[23] D. Taylor, Implanted component faults and their effects on gas turbine engine performance, *Journal of Engineering for Gas Turbines and Power*, 114 (1992) 110-116.

[24] A. Stamatis, K. Mathioudakis, G. Berios and K. Papailiou, Jet engine fault detection with discrete operating points gas path analysis, *Journal of Propulsion*, 76(1991) 1043–1048.

[25] T. Kobayashi and D. Simon, Hybrid neural-genetic algorithm technique for aircraft engine performance diagnostics, *Journal of Propulsion and Power*, 21(2005) 751-758.

[26] T. V. Groenstredt, A multipoint gas path analysis tool for gas turbine engines with a moderate level of instrumentation, *XV International Symposium on Air-Breathing Engines*, Bangalore, India, (2001) 1051 -1058.

[27] A. Gulati, D. Taylor and R. Sign, Multiple operating point analysis using genetic algorithm optimization for gas turbine diagnostic, *XV International Symposium on Air-Breathing Engines*, Bangalore, India, (2001) 1-8.

Appendix A

The PG9171E engine can be represented by a functional relation between quantities that defines the operating point, denoted by $\mathbf{u}$, quantities expressing components health, denoted by $\boldsymbol{X}$, and quantities measured for monitoring, denoted by $\mathbf{Y}$:

$$\mathbf{Y} = \mathrm{F}(\mathbf{u},\boldsymbol{X}) \tag{A-1}$$

A computerized engine model materializes such a relationship. For a given operating point, Eq. (A-1) can be simplified to:

$$\mathbf{Y} = \mathrm{F}(\boldsymbol{X}) \tag{A-2}$$

With an initial guessed parameter vector $\bar{\boldsymbol{X}}$, the engine model provides a predicted measurement vector $\bar{\mathbf{Y}}$. An optimization approach is applied to minimize an objective function as follows:

$$\text{Object Function} = \sum_i \phi(\left\|\bar{\mathbf{Y}}_i - \mathbf{Y}_i\right\|) \tag{A-3}$$

which is the function of the difference $\mathbf{e}$ between the real measurement vector $\mathbf{Y}$ and the predicted measurement vector $\bar{\mathbf{Y}}$. A minimization of the objective function is carried out iteratively until the best predicted engine component parameter vector $\bar{\boldsymbol{X}}$ for real $\boldsymbol{X}$ is obtained.

Di Xia received a B.S. degree in Mechanical Engineering from Tongji University and is currently a Ph.D. candidator at the School of Mechanical Engineering at Jiaotong University in Shanghai, China. Dr. Xia's research interests are in the area of gas turbine and gas path analysis.